

Origin and Size Distribution of Secondary Nuclei

Microscopic observations and Coulter counter measurements of the secondary nuclei produced when a parent crystal of potash alum was contacted with a solid rod suggest that these nuclei are born by an attrition mechanism which appears to be dependent on the growth rate of the crystal. The nuclei can be up to 50 μm in size. The nuclei smaller than about 4 μm are relatively insensitive to supersaturation, whereas the number greater than about 4 μm is approximately linear in supersaturation.

JOHN GARSIDE
I. T. RUSLI
and
M. A. LARSON

Department of Chemical Engineering
Iowa State University
Ames, Iowa 50011

SCOPE

Although secondary nucleation appears to be the major source of nuclei in industrial crystallizers, little is known about the mechanism by which such nuclei are produced. Scale-up of secondary nucleation kinetics is therefore difficult and is a major obstacle to the further application of population balance techniques to crystallizer design. Most of the published data on secondary nucleation kinetics have been obtained from observations on comparatively large crystals, nucleation rates then being inferred from the number of these crystals. Results of recent studies

showing anomalous growth behavior of small crystals imply that secondary nucleation rates measured in this way may seriously underestimate the true kinetics.

In the study reported here, the production of secondary nuclei as a result of contacting a solid rod with a crystal surface is observed directly using optical microscopy. In addition, the size distribution of secondary nuclei, within a few seconds of being produced from a parent crystal, is measured by using a Coulter counter.

CONCLUSIONS AND SIGNIFICANCE

Both the microscopic observations and the Coulter counter measurements indicate that secondary nuclei of potash alum are produced directly into size ranges up to 50 μm , although the majority are less than about 20 μm . The nuclei appear to be formed by an attrition mechanism in which particles are detached from the growing crystal surface. The number of nuclei produced depends on the supersaturation. Although the number and distribution of sizes less than about 4 μm is relatively independent of supersaturation, the total number greater than 4 μm in-

creases in an approximate linear manner with supersaturation, and more larger particles are produced at higher supersaturations.

Because of the ease with which nuclei appear to be produced by attrition, it is likely that nucleation rates in industrial crystallizers are dominated by such a mechanism. Successful scale-up, therefore, requires detailed knowledge of the relation between frequency and energy of crystal collisions and of the hydrodynamics of crystallizers and information describing the variation of nuclei production rate with energy of contact.

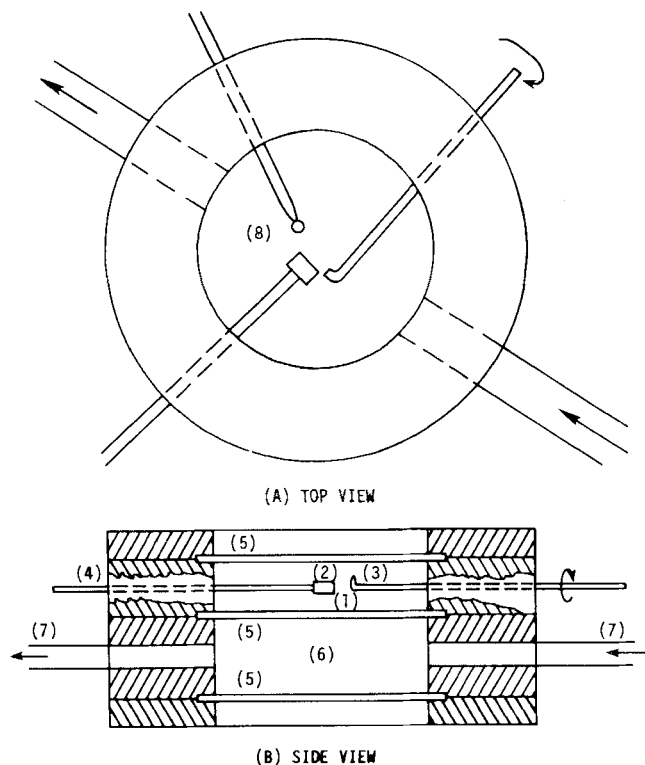
The process of secondary nucleation appears to be the major source of nuclei in industrial crystallizers. It is thus apparent that application of mathematical models to crystallizer design requires a knowledge of the way in which secondary nucleation kinetics vary with crystallizers operating parameters. Over recent years, many studies have been directed at understanding and explaining the phenomenon of secondary nucleation and measuring kinetic data. In spite of these studies, however, the mechanisms by which secondary nuclei are produced are still a matter of speculation.

J. Garside is at University College London, Torrington Place, London WC1 7JE, U.K.

0001-1541-79-9960-0057-\$01.05. © The American Institute of Chemical Engineers, 1979.

Recent reviews of secondary nucleation by Botsaris (1976) and Estrin (1976) have summarized the existing state of knowledge, and it is clear that a number of different mechanisms may produce secondary nuclei. Botsaris pointed out that the origin of secondary nuclei has been proposed as the crystal surface, a semioordered layer adjacent to the crystal surface or the supersaturated solution. Nuclei may then be removed from these sources in a number of ways, for example, by fluid shear or by collisions of a crystal with an external surface or another crystal. Alternatively potential nuclei may be activated in some way by increasing the effective local supersaturation around the crystal or by activating embryos in the bulk solution.

Most of the experiments that have contributed to such deductions and speculations have been such that second-



(1) Solution, (2) Parent crystal, (3) Contacting rod, (4) Support rod, (5) Cover glasses, (6) Constant temperature water, (7) Water inlet and outlet, (8) Thermistor

Fig. 1. Schematic diagram of cell used to observe secondary nucleation.

dary nucleation rates were estimated from the numbers of crystals growing to visible size. (See, for example, the frequently quoted works of Strickland-Constable, 1972, Lal et al., 1969, and Clontz and McCabe, 1971. A number of recent studies in continuous MSMPR crystallizers, for example, Youngquist and Randolph, 1972, Khambaty and Larson, 1978, and Jancic and Garside, 1976, have made use of a Coulter counter to measure crystal size distribution down 1 to 3 μm .) The result of such work provides indirect evidence that many secondary nuclei are born directly in to the size ranges between about 1 and 10 μm , although many of these secondary nuclei appear to grow very slowly. Other evidence suggests that the growth rate of many very small crystals is immeasurably small (Bujac, 1976; van't Land and Wienk, 1976), while direct growth kinetic measurements on potash alum (Garside and Jancic, 1976) show that 3 μm crystals appear to grow at one twentieth the rate of 70 μm crystals. Such results cast doubts on the validity of deriving fundamental information on secondary nucleation from observations of crystals that have grown to visible size. It may be, however, that those nuclei that do grow are the only effective ones in populating the larger size ranges and so are the only ones of real importance for the development of the crystal size distributions.

In this paper, we report work that attempts to provide more definitive evidence of the origin of secondary nuclei. Two separate experiments are reported. In the first, direct microscopic observation of a growing crystal face was made while the crystal was contacted with a metal rod. In the second, a Coulter counter was used to measure the number and size distribution of secondary nuclei produced by contacting a growing crystal with a rod.

The immediate size distribution of the secondary nuclei was measured and analyzed as a function of supersaturation. The subsequent behavior of these nuclei will be

considered in a subsequent paper. The system used in all these studies was potash alum-water, and all experiments were performed at 30.0°C.

DIRECT OBSERVATION OF SECONDARY NUCLEI PRODUCTION

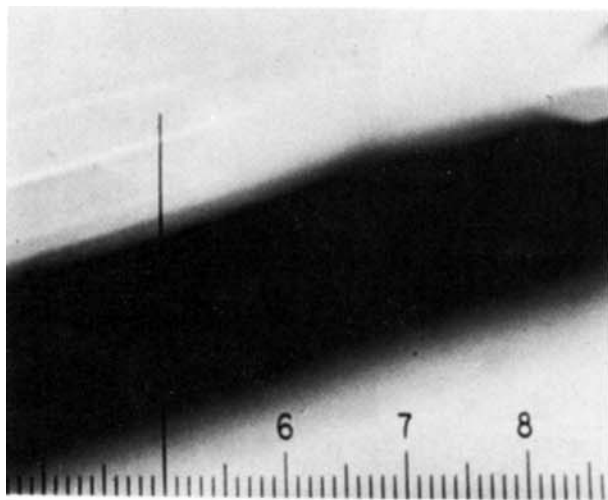
Experimental Procedure

Figure 1 shows the cell used for microscopic observation of a crystal surface while it was contacted by a solid rod. The cell was constructed of stainless steel, with upper and lower sections separated and sealed by circular cover glasses. Solution was held in the upper section which had a capacity of 5 ml. Thermostatically controlled water was circulated through the lower section to provide temperature control. A thermistor projecting to within 5 mm of the crystal was mounted in the upper section to measure the solution temperature. The crystal support rods and the contacting rod were made of stainless steel. The tip of the contacting rod was bent through 90 deg and shaped so that the contacting surface was flat. This surface approximated an equilateral triangle with side length of about 1 mm. The crystal was observed from above with transmitted light using an optical microscope with a magnification of $\times 100$. Photomicrographs were made of the contacting process, of the subsequent growth of the parent crystal, and of the nuclei produced by the contact. By using this technique, particles of 1 μm in size could be resolved.

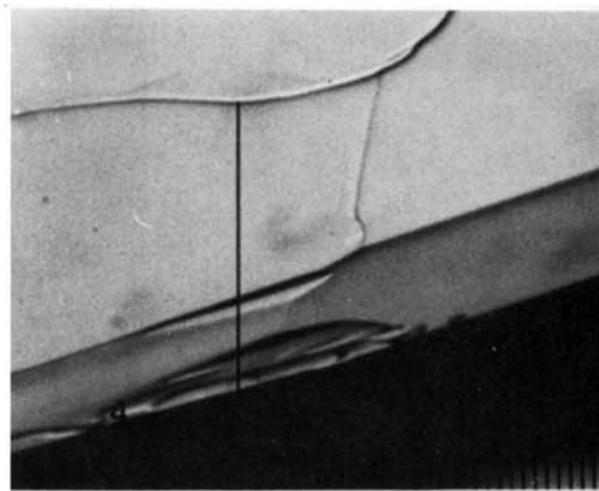
A crystal, about 3 mm in size, was fixed to the support rods using quick drying epoxy adhesive. It was then slightly dissolved with distilled water to remove any crystalline material adhering to the surface. Solutions of given concentrations were prepared by saturating at appropriate temperatures using analytical grade potash alum and distilled water. Corresponding solution concentrations were calculated using the solubility data of Jancic (1976). A solution of the desired concentration was then placed in the cell using a hypodermic syringe. The initial temperature of the solution and the thermostated water was 0.5°C above the solution saturation temperature. This temperature was maintained for 15 min during which time the crystal again dissolved slightly. The water temperature was then reduced to 30°C which corresponded to a known supersaturation in the solution. This cooling process took about 10 min, and then the solution was held at 30°C for about 15 min to allow the crystal to grow at the supersaturation used for the experiment. The crystal was then contacted by rotating the contacting rod about its axis. The energy of contact could not be measured, although it was certainly very small, and the contact could be more precisely defined as touching rather than striking. Observation of the crystal surface and of any nuclei produced was then continued for a period of time.

Results

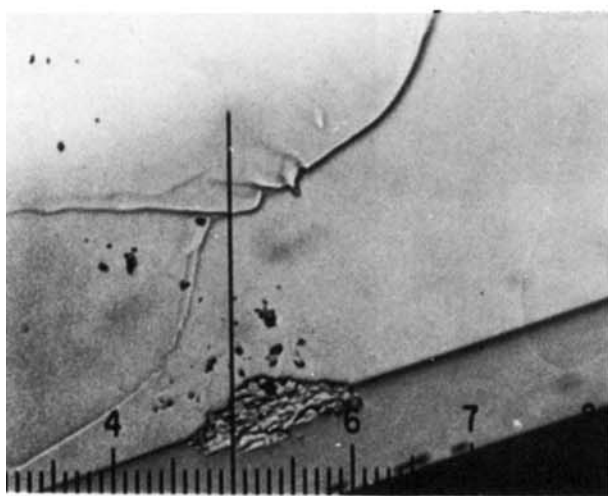
Figure 2 illustrates a typical sequence of photographs corresponding to a concentration driving force $\Delta c = 0.83$ g alum/100 g solution (that is, $\Delta T = 1.85^\circ\text{C}$, $\sigma = 0.058$). In (A), the crystal is dissolving and has rounded edges. After a period of growth (B), the edges are sharp, and a growth layer can be seen on the crystal face. The next photograph (C) was taken 1 min after the contact. The contact site is clearly visible and is about 120 μm across. Fragments from the crystal have been strewn around the damaged area, and many other fragments could also be seen on the base of the cell. These fragments are secondary nuclei, and they range in size from 1 to 15 μm . As time progressed, the crystal continued to grow and the surface healed, so that 13 min after the contact (F) the contact site showed few distinguishing features,



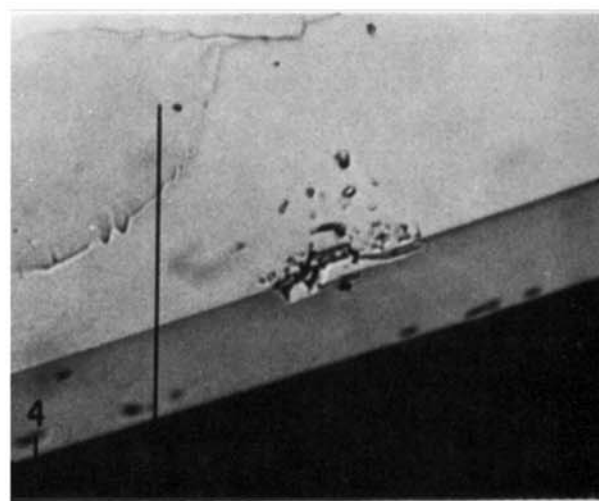
(A) INITIAL DISSOLUTION



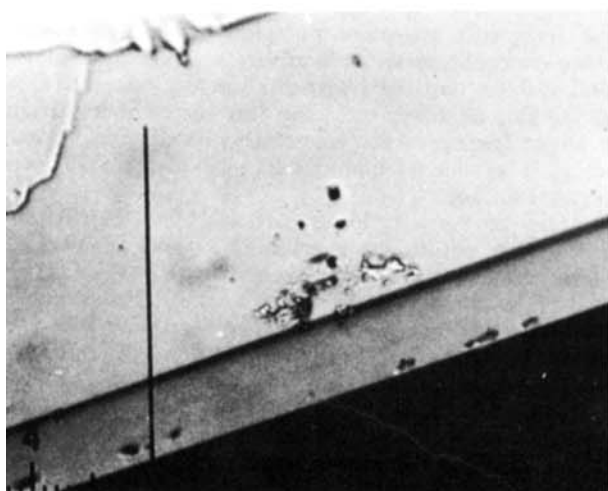
(B) GROWTH BEFORE CONTACT



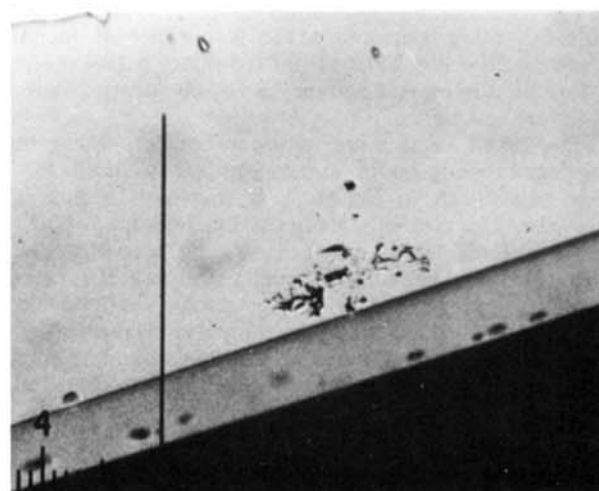
(C) 60 sec AFTER CONTACT



(D) 270 sec AFTER CONTACT



(E) 550 sec AFTER CONTACT

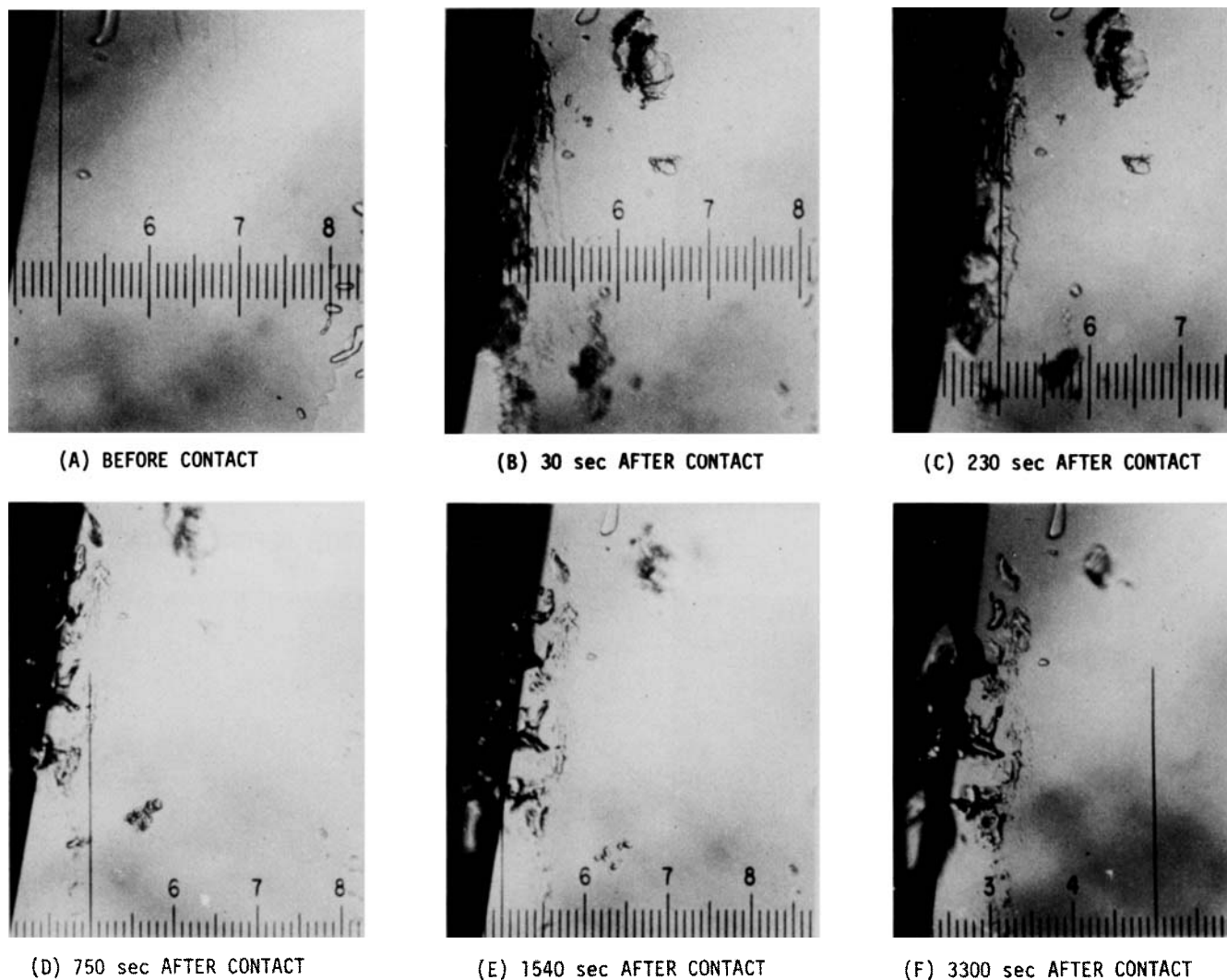


(F) 800 sec AFTER CONTACT

100 μm

$\Delta T = 1.85^{\circ}\text{C}$: $\Delta c = 0.83 \text{ g ALUM}/100 \text{ g SOLUTION}$: $\sigma = 0.058$

Fig. 2. Microscopic observation of secondary nuclei (1).



$\Delta T = 1.85^{\circ}\text{C}$; $\Delta c = 0.83 \text{ g ALUM}/100 \text{ g SOLUTION}$; $\sigma = 0.058$

Fig. 3. Microscopic observation of secondary nuclei (II).

although there appeared to be a number of inclusions present at the site. Most of the secondary nuclei originally sitting on the crystal surface had been incorporated into the growing face.

The result of a more vigorous contact, made under the same condition of supersaturation as used for the sequence shown in Figure 2, is shown in Figure 3. In this case, the area of damage is much larger, about 300 μm in length. Many of the resulting secondary nuclei are also much larger with fragment up to 50 μm being visible. The larger fragments appear somewhat platelike.

Sequences similar to those shown in Figures 2 and 3 but obtained under different conditions of supersaturation were also taken, and these will be published elsewhere (Garside and Larson, 1978). The main conclusions that can be drawn from all the observations may be summarized as follows:

1. Crystal fragments or secondary nuclei are produced in both under and supersaturated solutions.
2. In undersaturated solutions ($\Delta T = -0.5^{\circ}\text{C}$), these fragments are within the size range 1 to 5 μm . They rapidly dissolve, as does the site of the contact on the crystal face.
3. In supersaturated solutions, larger fragments are produced in addition to the smaller fragments. These

larger fragments are more numerous when the contact is more energetic or when it covers a larger area of the crystal surface, and the fragments range in size up to at least 50 μm , although most are less than about 20 μm . The larger fragments are frequently platelike in appearance, as if a slice of material had been detached from the crystal surface.

4. Many of the very small particles (less than 5 μm) appear either not to grow or to grow very slowly. All the larger fragments, however, seem to grow.

5. Gentle contact with a dry crystal also produces crystals up to about 5 μm in size.

NUMBER AND SIZE DISTRIBUTION OF SECONDARY NUCLEI

Experimental Procedure

To complement the qualitative observations described above, measurements were made of the number and size distribution of secondary nuclei produced by contacting a crystal with a metal rod.

A jacketed glass vessel was used as a batch crystallizer as shown in Figure 4. It was similar in design to that used by Garside and Jancic (1976) but had a slightly greater capacity of 400 ml. In addition to a Coulter

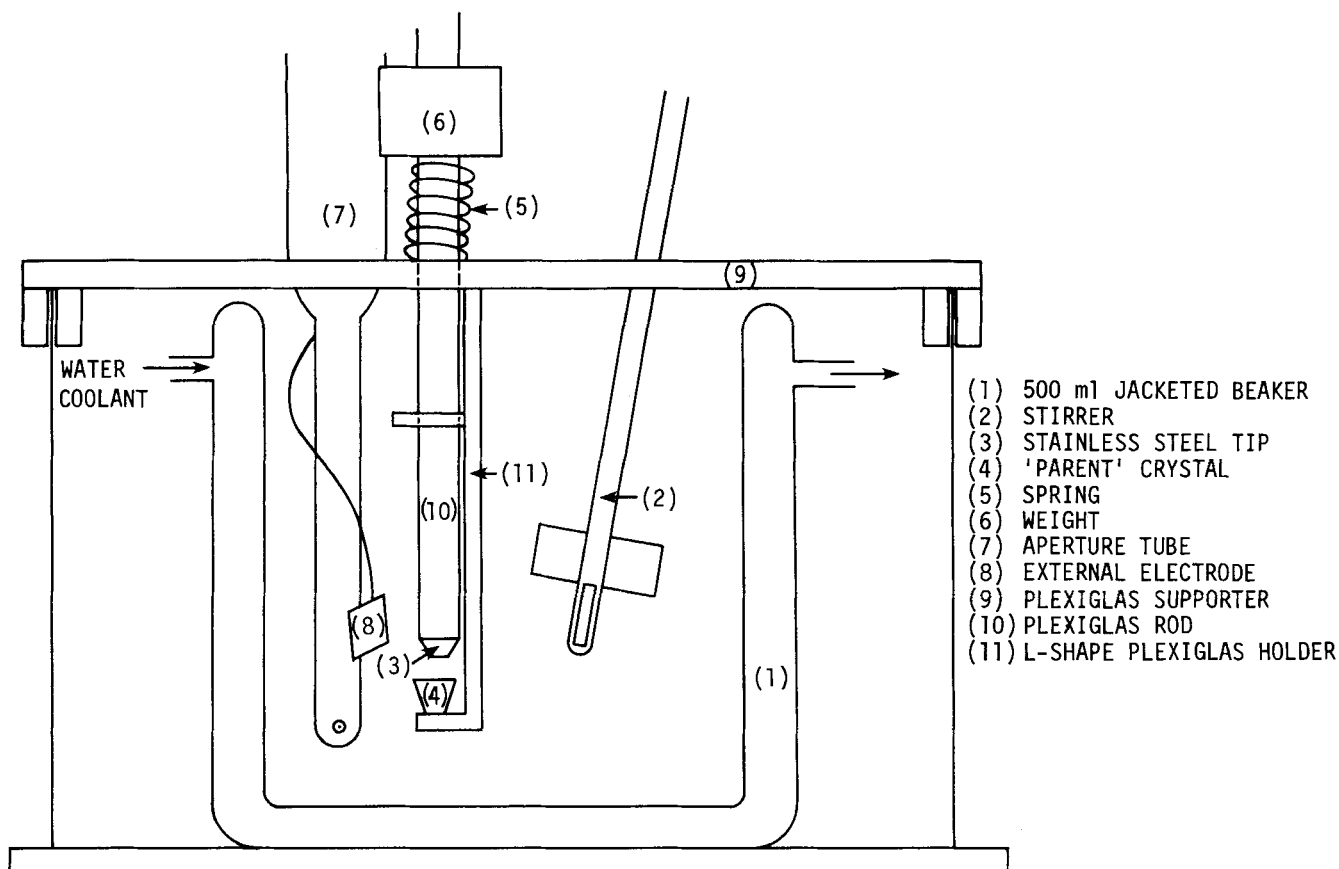


Fig. 4. Experimental apparatus.

counter sampling tube and a stirrer, a crystal contactor as used by Larson and Bendig (1976) was placed in the crystallizer. This contactor was operated manually rather than by an electrical relay as in the original design. A model TA II Coulter counter was used to measure the size distribution of secondary nuclei.

Saturated solutions of a given temperature were prepared as described earlier in the microscopic experiments. Before the start of a run, the solution, at a temperature of about 3.5°C above the saturation temperature, was filtered several times through a 0.2 μm filter. Constant temperature water at 1.5°C above the saturation temperature was circulated through the water jacket of the crystallizer. Approximately 300 ml of the solution were transferred to the crystallizer, and the circulating water temperature was then reduced to 0.5°C above the saturation temperature. The stirrer speed was 150 rev/min for all runs.

In the meantime, the parent crystal (about 10 mm in size) was mounted on a L shaped Plexiglas support and was pretreated by dissolution in a slightly undersaturated solution for about 5 min. When the temperature of the solution in the crystallizer reached 0.5°C above the saturation temperature, the parent crystal was immersed in the solution to allow further slight dissolution. The temperature was then further reduced to 30.0°C at the rate of approximately 0.2°C/min. When the temperature reached 30.0°C, several readings of the Coulter counter background count were taken. If these background readings were satisfactory (being relatively low and constant), five contacts were made in quick succession, the total time to make these contacts being about 10 s. Five contacts were necessary in order to produce enough particles for a significant count to be made. The initial size dis-

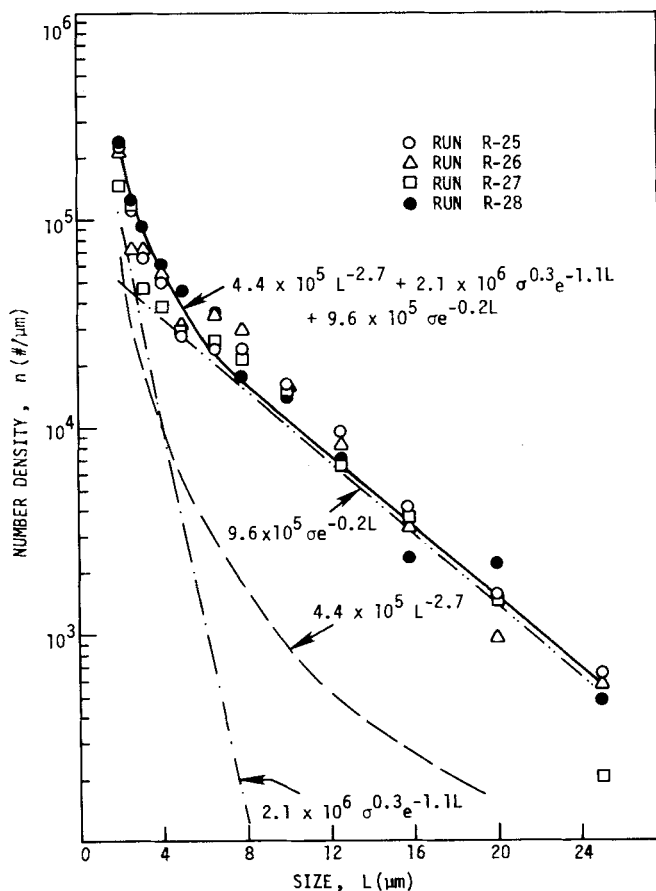


Fig. 5. Initial nuclei size distribution for $\sigma = 0.08$ ($\Delta T = 2.6^\circ\text{C}$, $\Delta C = 1.13$ g potash alum/100 g solution).

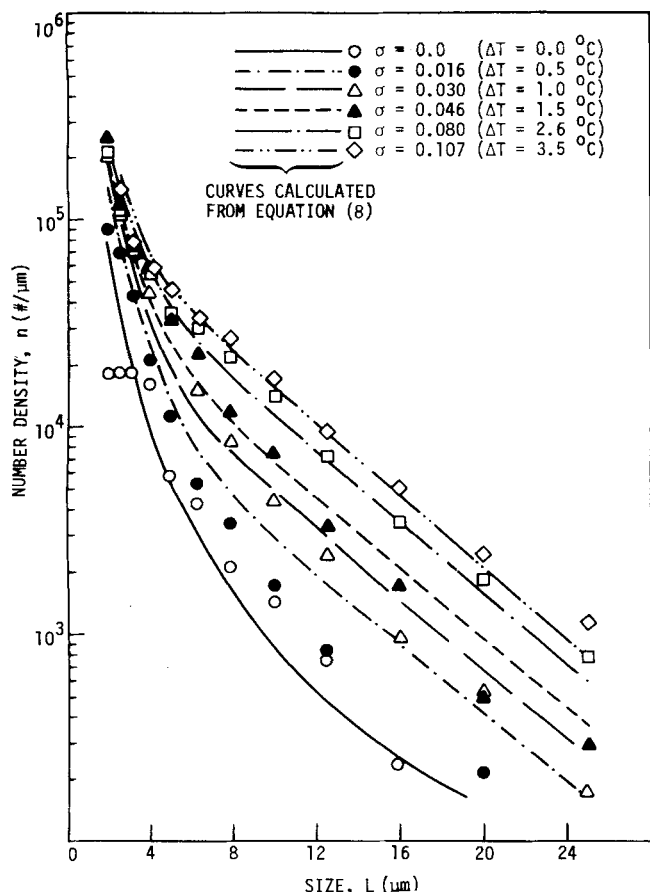


Fig. 6. Initial nuclei size distribution for various supersaturations.

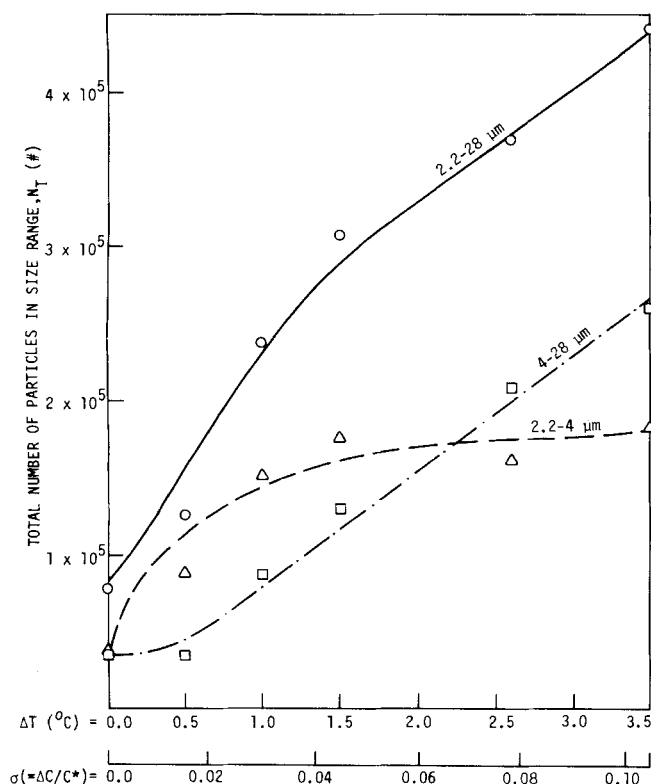


Fig. 7. Total number of secondary nuclei produced for three size ranges.

tribution of secondary nuclei produced by the contacts was then measured within 1 min of the contacts.

Throughout the experimental run, it was necessary to flush and replace the solution inside the aperture tube with solution from a reservoir kept at about 1° to 2°C above the supersaturation temperature. This process was done approximately every 5 min and more frequently when the solution was supersaturated. The purpose was to prevent crystallization inside the aperture tube which would affect the Coulter counter readings.

Measurements were made in saturated and supersaturated solutions covering the range of concentration driving force Δc up to 1.52 g potash alum/100 g solution ($\sigma = 0.107$) which corresponds to a maximum ΔT of 3.5°C. A 70 μm orifice tube was used for values of Δc up to 1.13 g potash alum/100 g solution, so enabling the size distribution to be made over the range of 1.7 to 28 μm . At higher supersaturations, the large particles produced by the contacts rapidly blocked this orifice, and a 100 μm orifice tube was used. The corresponding lower size limit measured was 2.2 μm . The area of contact was estimated to be about 3.1 mm^2 . The energy of contact was estimated to be about 8×10^4 erg.

More detailed discussion of this procedure and equipment is given by Rusli (1977).

Results

The size distribution data from the Coulter counter were evaluated in terms of number density (see the discussion by Randolph and Larson, 1971). Since nucleation occurs only when the parent crystal is contacted, and since it is unlikely that each contact produced the same number and size distribution of nuclei, the number density is evaluated in terms of the total number of nuclei produced by five contacts. In this paper, the discussion will be concerned mainly with the initial size distributions. These size distributions were the first readings taken from the Coulter counter within 1 min of the contacts.

The initial size distribution of secondary nuclei produced at $\Delta c = 1.13$ g potash alum/100 g solution ($\Delta T = 2.6^\circ\text{C}$) is shown in Figure 5. The results of four separate experiments performed under identical conditions are shown to illustrate the reproducibility of the data. These sets of data are typical of results obtained at other supersaturations. Results for other values of Δc are given in Figure 6 in which only the average values are shown.

For condition of saturation and supersaturations up to about $\Delta T = 1^\circ\text{C}$, the numbers of secondary nuclei in all size ranges increase with increasing ΔT . At higher values of supersaturation ($\Delta T > 1.0^\circ\text{C}$), the numbers of nuclei at sizes less than about 4 μm appear to be fairly constant with supersaturation. The number of particles in the larger size ranges, however, continues to increase with increasing Δc . This trend can be seen more clearly in Figure 7 which shows the total number of particles produced as a function of concentration driving force and the total number of particles less than and greater than 4 μm . The significant increase in the number of larger particles at higher supersaturations compared with the constant numbers of the smaller particles is evident.

The initial size distribution data were fitted to an empirical model equation describing the effects of supersaturation and size on number density. Other factors which might affect the number density, for example, fluid velocity, energy and area of contacts, frequency of contacts, etc., were assumed constant. Thus

$$n = f(L, \sigma) \quad (1)$$

A supersaturation function that gave a nonzero value at the saturation point ($\sigma = 0.0$) is required to describe

the experimental data, and Equation (2) was found to be satisfactory:

$$n(L, \sigma) = C_1(L) + C_2(L)\sigma^a \quad (2)$$

The size dependent function $C_1(L)$ can be obtained from the number density for $\sigma = 0.0$. The data were found to be satisfactorily fitted by an equation of the form

$$C_1(L) = k_1 L^{-b} \quad (3)$$

and, using least-square regression analysis, we found the numerical values to be

$$C_1(L) = 4.4 \times 10^5 L^{-2.7} \text{ \#}/\mu\text{m} \quad (4)$$

The curve represented by Equation (4) is shown in Figure 6 for $\sigma = 0.0$. It is a reasonable representation of the data over the size range measured in this experiment, that is, from 2 to 25 μm .

Since the effects of both supersaturation and size on number density are different for the small size range ($2 < L < 4 \mu\text{m}$) and for the large size range ($4 \leq L < 25 \mu\text{m}$), the experimental results for these two size ranges were fitted separately to Equation (2). Except for different values of the constants, each size range can be separately represented by the same form of Equation (5):

$$n(L, \sigma) = 4.4 \times 10^5 L^{-2.7} + k_2 \sigma^a e^{-mL} \text{ \#}/\mu\text{m} \quad (5)$$

The numerical values of the constants for each size range are

$$n(L, \sigma) = 4.4 \times 10^5 L^{-2.7} + 3.0 \times 10^6 \sigma^{0.3} e^{-1.1L} \text{ \#}/\mu\text{m} \quad \text{for } 2 < L < 4 \mu\text{m} \quad (6)$$

$$n(L, \sigma) = 4.4 \times 10^5 L^{-2.7} + 9.6 \times 10^5 \sigma e^{-0.2L} \text{ \#}/\mu\text{m} \quad \text{for } 4 \leq L < 25 \mu\text{m} \quad (7)$$

It should be noted that the second term in Equation (6) indicates that the number density increases slightly with supersaturation whereas the experimental data were approximately constant at σ greater than 0.03 ($\Delta T = 1.0^\circ\text{C}$). Further, the average slope of the experimental data for larger sized nuclei shows slight dependence on σ which might suggest an exponential function with respect to both size and supersaturation in Equation (7). Owing to the experimental scatter and limited data available, however, it does not seem appropriate at this stage to attempt more complicated expressions. The important point which should be emphasized is that there seem to be two different kinds of nuclei produced, the small size nuclei ($2 < L < 4 \mu\text{m}$) in which the number of nuclei produced is a weak function of supersaturation and the larger size nuclei ($4 \leq L < 25 \mu\text{m}$) in which the number of nuclei produced is significantly dependent on supersaturation.

It is possible to combine Equations (6) and (7) to give one equation which covers the size range between 2 and 25 μm . Thus

$$n(L, \sigma) = 4.4 \times 10^5 L^{-2.7} + 2.1 \times 10^6 \sigma^{0.3} e^{-1.1L} + 9.6 \times 10^5 \sigma e^{-0.2L} \text{ \#}/\mu\text{m} \quad \text{for } 2 < L < 25 \mu\text{m} \quad (8)$$

The last two terms in Equation (8) represent the asymptotic lines for the small and large size ranges, respectively. The curves represented by Equation (8) are shown in Figure 6 where they are compared with the experimental data. In addition, each term on the right-hand side of Equation (8) is shown separately in Figure 5 for illustration. Note that the coefficient of the second term in Equation (6) has been slightly adjusted to account for the contribution from the last term in Equation (8) which becomes significant ($\sim 30\%$) for the small size range at high supersaturations (as shown in Figure 5). Unless otherwise stated, Equation (8) will be used as the model equation to represent initial nuclei size distribution.

DISCUSSION

It is clear from the microscopic observations that large numbers of secondary nuclei can be produced by direct attrition of a crystal surface. The energy of contact required to produce such nuclei can be very small, certainly far less than that used in most previous secondary nucleation studies, for example, Clontz and McCabe (1971) and Larson and Bendig (1976), and indeed less than that used in the second series of experiments described here.

Both series of experiments showed that secondary nuclei resulting from attrition or breakage processes are formed at sizes as small as 1 to 2 μm , the limits of detection with the techniques employed. Although it is likely that smaller secondary nuclei are also formed, concepts used to describe the breakage of particles suggest that in a given breakage event, fragments are only formed down to some minimum size (Lowrison, 1974). If similar mechanisms are applicable to an attrition mechanism for the secondary mechanism, then nuclei may only be produced down to some finite size which could well be on the order of 1 μm .

The effect of supersaturation appears to be different for the smaller microparticles (less than about 4 μm) and for the larger macroparticles (greater than about 4 μm). The total number and size distribution of the microfragments is comparatively insensitive to supersaturation, and the total number of fragments born into the size range 2 to 4 μm is virtually constant for values of Δc above about 0.4 g alum/100 g solution (see Figure 7). These microfragments perhaps then result from a mechanism unrelated to a growth or nucleation process and may, for example, either be produced by an attrition mechanism or may break away from the crystal surface at the point where the larger fragments are detached.

Both series of experiments also showed that comparatively large secondary nuclei can be produced. The number and size distribution of the macrofragments depend on supersaturation. The total number produced is approximately linear with supersaturation (see Figure 7), and these increasing numbers of particles are produced over the entire size range above about 4 μm . The microscopic observation showed that very large particles, up to at least 50 μm , can sometimes be produced. Although the Coulter counter only measured the size of particles up to about 25 μm , the increasing numbers of large particles at higher supersaturations were confirmed by the experimental difficulty encountered when using a 70 μm orifice under these conditions. This orifice rapidly became blocked, and a 100 μm orifice had to be used.

Previous workers have suggested that there may be a link between the rate of secondary nucleation and the kinetics of crystal growth and that the two processes sometimes appear to show the same order dependence on supersaturation. To some extent, the present results confirm this hypothesis in that the kinetics of growth of small potash alum crystals are also linear in supersaturation (Garside and Jancic, 1976), although the growth kinetics of larger alum crystals depend on supersaturation to a power closer to 2 (Garside et al., 1975). Nevertheless, the microscopic observations showed quite clearly that large particles are produced by a fracture or attrition mechanism. Such breakage appeared to be easier at an edge of the crystal, although breakage at the center of a face was still surprisingly easy. Crystal fragments often seemed to flake off the face. This may have occurred because of one mechanism which involved the breakage of a solid crystalline skin covering a solution inclusion. Such inclusions were visible under the microscope and would form weak points in the crystal surface. The number of inclusions generally increases with the

rate of crystal growth and hence with supersaturation, and so secondary nuclei produced by such a mechanism may be expected to show a supersaturation dependence similar to the growth rate.

The structure of the crystal surface also depends on supersaturation. In general, the crystal surface will tend to become molecularly rough at higher supersaturations, provided that the relative binding energy of the structural units in the surface are not too high compared to the binding energy between the crystal surface and the fluid. These energies can be quantified by the α factor as discussed by, for example, Jackson (1958) and Bennema and Gilmer (1973). Such theories, however, refer to roughness on the molecular scale, and it is difficult to see how such effects are relevant to the type of secondary nucleation observed here. The surface structure of the alum crystals did not appear to change on a microscopic scale as a result of supersaturation changes, and so for this case, at least, such effects are probably not important.

One of the most persuasive hypotheses describing the supersaturation dependence of secondary nucleation is the survival theory of Strickland-Constable (1972). In this, the initial production of nuclei is envisaged as being in the range of the critical size. This initial distribution is assumed to be independent of the supersaturation. Since the critical size decreases with increasing supersaturation, the number of surviving nuclei increases with increasing supersaturation, resulting in the observed dependence on supersaturation. Such a mechanism does not seem to be of importance in the work reported here. Neither do any of the other speculative mechanisms mentioned in the introduction to this paper and summarized by Botsaris (1976) and Estrin (1976), for example, those involving semiordered layers, solute clusters, or activated embryos. Attrition of the crystal surface and the instantaneous production of nuclei having a spectrum of sizes seem sufficient to explain the observations. The subsequent growth of these nuclei will then determine the apparent nucleation rate as deduced from observations of larger crystals. This growth behavior will be discussed in a subsequent paper.

A consequence of this mechanism of secondary nucleation, and especially of the ease with which secondary nuclei are produced, is that nucleation rates in industrial crystallizers will be dominated by those nuclei produced as a result of crystal collisions. In many cases, it seems probable that this is the only significant source of nuclei. Successful scale-up of nucleation kinetics will, therefore, demand a greater understanding of the factors relating the frequency and energy of crystal collisions to the hydrodynamics of crystallizers. In addition, the relation between contact energy and the number of nuclei produced needs to be more fully understood. Reductions in nucleation rates, observed when impellers and crystallizer surfaces have been coated with soft materials (for example, Evans et al., 1974), can be easily explained on the basis of the attrition mechanisms discussed here. Such techniques probably offer real value in industrial situations where nucleation rates are excessive.

ACKNOWLEDGMENT

The authors wish to acknowledge the support of the Iowa State University Engineering Research Institute and the National Science Foundation through Grant ENG 77-06054 for their support of this work.

NOTATION

- a = constant in Equation (2)
 b = constant in Equation (3)
 c = solution concentration (g alum/100 g solution)

- c^* = saturation concentration (g alum/100 g solution)
 Δc = concentration difference ($= c - c^*$) (g alum/100 g solution)
 $C_1 C_2$ = size dependent functions in Equation (2)
 m = constant in Equation (5)
 L = crystal size (μm)
 n = population density ($\#/\mu\text{m}$)
 ΔT = temperature difference between saturation and solution temperature ($^{\circ}\text{C}$)
 σ = supersaturation $(c - c^*)/c^*$

LITERATURE CITED

- Bennema, P., and G. H. Gilmer, "Kinetics of Crystal Growth," in *Crystal Growth: An Introduction*, P. Hartman, ed., Chapt. 10, North Holland, Amsterdam (1973).
Botsaris, G. D., "Secondary Nucleation, A Review," in *Industrial Crystallization*, J. W. Mullin, ed., p. 3, Plenum Press, New York (1976).
Bujac, P. D. B., "Attrition and Secondary Nucleation in Agitated Crystal Slurries," *ibid.*, p. 23 (1976).
Clontz, N. A., and W. L. McCabe, "Contact Nucleation of Magnesium Sulfate," *Chem. Eng. Progr. Symposium Ser. No. 110*, 67, 6 (1971).
Estrin, J., "Secondary nucleation—A Review," in *Preparation and Properties of Solid State Materials*, W. R. Wilcox, ed., Marcel Dekker, New York (1976).
Evans, T. W., G. Margolis, and A. F. Sarofim, "Mechanism of Secondary Nucleation in Agitated Crystallizers," *AIChE J.*, 20, 950 (1974).
Garside, J., and S. J. Jancic, "Growth and Dissolution of Potash Alum Crystals in the Subsieve Size Range," *ibid.*, 22, 887 (1976).
Garside, J., R. Janssen-Van Rosmalen, and P. Bennema, "Verification of Crystal Growth Rate Equations," *J. Cryst. Growth*, 29, 353 (1975).
Garside, J., and M. A. Larson, "Direct Observation of Secondary Nuclei Production," *J. Cryst. Growth* 43, 694 (1978).
Jackson, K. A., "Mechanisms of Growth," in *Liquid Metals and Solidification*, p. 174, American Society for Metals, Cleveland, Ohio (1958).
Jancic, S. J., Ph.D. thesis, "Crystallization Kinetics and Crystal Size Distributions in Mixed Suspension Mixed Product Removal Crystallizers," University of London, England (1976).
———, and J. Garside, "A New Technique for Accurate Crystal Size Distribution Analysis in an MSMPR Crystallizer," in *Industrial Crystallization*, J. W. Mullin, ed., p. 363, Plenum Press, New York (1976).
Khambaty, S., and M. A. Larson, "Crystal Regeneration and Survival of Small Crystals in Contact Nucleation," *Ind. Eng. Chem. Fundamentals* 17, 160 (1978).
Lal, D. P., R. E. A. Mason, and R. F. Strickland-Constable, "Collision Breeding of Crystal Nuclei," *J. Cryst. Growth*, 5, 1 (1969).
Larson, M. A., and L. L. Bendig, "Nuclei Generation from Repetitive Contacting," *AIChE Symp. Ser. No. 153*, 72, 21 (1976).
Lowrison, G. C., *Crushing and Grinding*, Butterworth, London (1974).
Randolph, A. D., and M. A. Larson, *Theory of Particulate Processes*, Academic Press, New York (1971).
Rusli, I. T., M.S. Thesis, "Origin Size Distribution and Growth of Small Crystals in Contact Nucleation," Iowa State University of Science and Technology, Ames, Iowa (1977).
Strickland-Constable, R. F., "The Breeding of Crystal Nuclei—A Review of the Subject," *AIChE Symp. Ser. No. 121*, 68, 1 (1972).
Van't Land, C. M., and B. G. Wienk, "Control of Particle Size in Industrial NaCl—Crystallization," *Industrial Crystallization*, J. W. Mullin, ed., p. 51, Plenum Press, New York (1976).
Youngquist, G. R., and A. D. Randolph, "Secondary Nucleation in a Class II System," *AIChE J.*, 18, 421 (1972).

Manuscript received March 13, 1978; revision received August 7, and accepted August 25, 1978.